Electrochemistry Communications 120 (2020) 106846

Contents lists available at ScienceDirect

Electrochemistry Communications

journal homepage: www.elsevier.com/locate/elecom

Electrochemical synthesis of carbon-metal fluoride nanocomposites as cathode materials for lithium batteries

M. Helen[a], Maximilian Fichtner[b,c], M. Anji Reddy[a,*]

[a] College of Engineering, Swansea University, Fabian Way, Swansea SA1 8EN, United Kingdom
[b] Helmholtz Institute Ulm (HIU), Electrochemical Energy Storage, Helmholtzstraße 11, 89081 Ulm, Germany
[c] Institute of Nanotechnology, Karlsruhe Institute of Technology, P.O. Box 3640, D-76021 Karlsruhe, Germany

ARTICLE INFO

Keywords:
CF_x
Metal fluorides
C-FeF_2 and C-NiF_2
Lithium batteries
Electrochemical synthesis

ABSTRACT

Herein we have demonstrated an electrochemical method for the synthesis of carbon-metal fluoride nanocomposites (CMFNCs). Electrochemical intercalation of transition metal ions into graphite fluoride (CF_x) resulted in the formation of CMFNCs. As a proof-of-concept, we have synthesized C-FeF_2 and C-NiF_2 nanocomposites by the electrochemical intercalation of Fe^{2+} and Ni^{2+} into CF_x from corresponding non-aqueous electrolytes. The C-FeF_2 and C-NiF_2 nanocomposites synthesized by this method showed high reversible capacity and cycling stability compared to chemically synthesized analogs as cathode materials for lithium batteries. The reversible capacity of chemically synthesized C-FeF_2 is 181 mAh g^{-1}, whereas electrochemically synthesized material is 349 mAh g^{-1} after 20 cycles. The better cycling performance of electrochemically synthesized C-FeF_2 was attributed to the homogeneous distribution of FeF_2 nanoparticles within the carbon matrix enabled by the electrochemical intercalation of Fe^{2+}. The electrochemical method described here is emission-free, cost-effective, occurs at room temperature, and extendable to the synthesis of several other CMFNCs. Moreover, it might provide new avenues for the synthesis of advanced functional materials.

1. Introduction

Metal fluorides are an important class of cathode materials for rechargeable lithium batteries due to their high energy density compared to the conventional insertion-based electrode materials [1–3]. However, metal fluorides are electrical insulators and show large volume changes during lithiation and delithiation reactions, which leads to gradual isolation of metal fluoride particles and results in capacity fading. Further, the electrochemical reaction between lithium and conversion-based metal fluorides is slow; therefore, crystallite size of the metal fluorides should be in the nanometer-regime to minimize the reaction path length of metal fluorides with lithium. In a tradeoff, the use of carbon-metal fluoride nanocomposites (CMFNCs) were suggested rather than using pure metal fluorides [4]. Indeed, these CMFNCs showed better cycling stability compared to pure metal fluorides [4,5]. However, the synthesis of CMFNCs is challenging. Often, mechanical milling was used to synthesize the CMFNCs [6]. But the mechanical milling breaks the electronic network of carbon and reduces the total electrical conductivity of the resulting composites. This results in poor cycling stability [6]. Alternatively, several chemical methods were suggested for the synthesis of CMFNCs [7–15]. Recently we have reported a one-step facile chemical redox method for the synthesis of CMFNCs [16–19]. The reaction of $Fe(CO)_5$, with graphite fluoride (CF_x) at 250 °C resulted in the formation of C-FeF_2 nanocomposites [16–19]. This method can be applied for the synthesis of various other CMFNCs (C-CoF_2, C-MoF_3) other than C-FeF_2, by simply changing the metal carbonyl precursor [18]. In addition to metal fluorides, we could also synthesize C-FeO_x and C-FeS nanocomposites by changing the reactant from CF_x to graphite oxide (CO_x) and sulphur-infused ultramicroporous carbon (C-S_x) [18]. This method produced quality CMFNCs but releases carbon monoxide (GO_x) as a side product, which is undesirable. Here we report an advanced electrochemical method for the synthesis of CMFNCs. Electrochemical intercalation of Fe^{2+} and Ni^{2+} into CF_x resulted in the electrochemical synthesis of C-FeF_2 and C-NiF_2 nanocomposites, which showed superior electrochemical performance as cathode materials for lithium batteries. The electrochemical method described here do not release any gas (emission-free), occurs at room temperature (RT), cost-effective, and extendable to the synthesis of several other CMFNCs.

* Corresponding author.
E-mail address: a.r.munnangi@swansea.ac.uk (M. Anji Reddy).

https://doi.org/10.1016/j.elecom.2020.106846
Received 24 August 2020; Received in revised form 8 September 2020; Accepted 22 September 2020
Available online 25 September 2020

2. Experimental section

Iron(II) perchlorate hydrate ($Fe(ClO_4)_2{\cdot}xH_2O$ – 98%), nickel(II) perchlorate hexahydrate ($Ni(ClO_4)_2{\cdot}6H_2O$), CF_x, anhydrous acetonitrile (ACN), and anhydrous tetrahydrofuran (THF) were obtained from Sigma Aldrich. Fe, Ni, and Li foils were obtained from Goodfellow. The Li electrolyte 1.0 M $LiPF_6$ in 1:1 ethylene carbonate (EC)/dimethyl carbonate (DMC) (LP30) was obtained from Merck. Fe and Ni electrolytes were made by dissolving required amounts of perchlorate salts (to prepare 1.0 M electrolytes) in ACN or THF. Activated molecular sieves (3 Å) were added to these electrolytes to absorb the H_2O molecules present in the perchlorate salts. The carbon content in the CF_x sample was estimated by elemental analysis, and the composition was determined as $CF_{1.1}$. Electrode fabrication and assembly of electrochemical cells was done in an argon-filled glove box. The electrodes were fabricated by mixing the active material, acetylene black and polyvinylidene fluoride (PVDF) in the mass ratio of 70:20:10. A slurry containing the above mixture was prepared by using N-methyl-2-pyrrolidinone (NMP), spread on stainless steel (SS) foil (area: 1.13 cm^2), and dried on a hot plate at 120 °C for 12 h. Typically, each electrode contained 2–3 mg of the active material (CF_x). The discharged electrodes collected from the corresponding cells were washed with anhydrous acetonitrile and dried at RT and used further in Li-half cells. The mass loading of FeF_2 or NiF_2 was calculated as follows. 1.0 mol of $CF_{1.1}$ would react with 0.5 mol of Fe. This results in the formation of $C(FeF_2)_{0.55}$. The weight percent of FeF_2 in $C(FeF_2)_{0.55}$ is approximately 80%. Each electrode contains 2.0 to 3.0 mg of $CF_{1.1}$, which results in the mass loading of 1.6 to 2.4 mg of FeF_2 in the electrode. Fe, Ni, and Li foils were used as the negative electrodes in respective cells, and a borosilicate glass fiber sheet saturated with respective electrolyte was used as separator and electrolyte. The cells were placed in an incubator (Binder) to maintain a constant operating temperature of 25 °C. The electrochemical studies were carried out using the Arbin battery cycling unit.

X-ray diffraction (PXRD) patterns were recorded using a Philips X'pert diffractometer equipped with Mo K_α radiation. In the case of CF_x electrodes, XRD patterns were collected on the electrodes after discharging the electrodes in Fe cells. The discharged $CF_{1.1}$ electrodes were collected from the corresponding cells washed with anhydrous acetonitrile and dried at RT. Scanning electron microscopy (SEM) was performed with a LEO 1530 at 15 keV using carbon tape as a substrate. Electrochemical studies were performed in Swagelok® type cells. Transmission electron microscopy was carried out on an aberration (image) corrected Titan 80–300 (FEI Company) operated at 80 kV equipped with a Gatan imaging filter Tridiem 863. The material for TEM studies consisted of powder sample free from solvents.

3. Results and discussion

CF_x is a primary lithium battery cathode material [20]. With an average discharge potential of 2.5 V vs. Li^+/Li and a theoretical specific capacity of 896 mAh g^{-1} (by assuming the electrochemical reaction of 1.1Li), CF_x is a viable cathode material for primary lithium batteries (Fig. 1a). Though the experimentally observed reduction potential of CF_x is 2.5 V vs. Li^+/Li, the thermodynamic reduction potential of CF_x is 4.21 V vs. Li^+/Li [21]. This high reduction potential of CF_x makes it thermodynamically feasible for Fe^{2+} and Ni^{2+} intercalation. Apart from its high reduction potential, CF_x also has other advantages as a reactant for the synthesis of CMFNCs. CF_x is a source of both carbon and fluorine. The insulating sp^3 - hybridized carbon in CF_x can be reduced to conductive sp^2 carbon upon the deintercalation of fluorine (reduction). Different types of CMFNCs can be synthesized by opting for CF_x

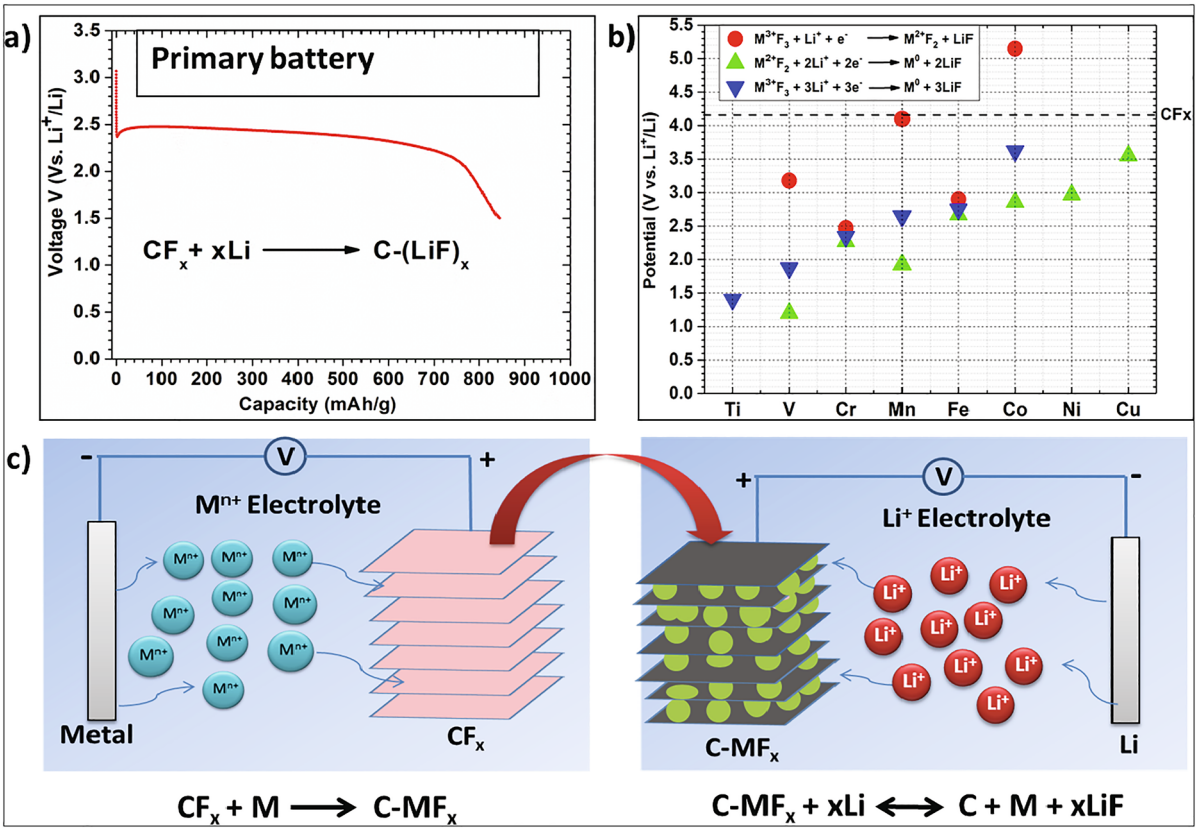

Fig. 1. a) discharge profile of CF_x/Li cell; b) formation potentials of various metal fluorides and $CF_{1.1}$ vs. Li^+/Li; c) schematic representation of the electrochemical approach used for the synthesis and testing of C-FeF_2 and C-NiF_2 nanocomposites.

with varying backbones of carbon [19] and further by different carbon to fluorine ratio [17].

The electrochemical reaction of Li with CF_x results in the formation of LiF crystallites embedded in the carbon matrix. In principle, the process is extendable for the synthesis of transition metal fluorides embedded in a carbon matrix by replacing the Li metal and Li-ion transporting electrolyte with the desired metal and metal-ion transporting electrolyte. Here, we demonstrate such an electrochemical reaction is indeed extendable to the synthesis of other metal fluorides (FeF_2 and NiF_2). Lithium exists as a monovalent (Li^+) in the intercalated state. But Fe and Ni can exist in several oxidation states. Therefore, these transition metal ions might have different oxidation states after the intercalation due to the possible internal redox reactions with the host, which highly depends on the host material. In these studies, we assume Fe and Ni are intercalated as Fe^{2+} and Ni^{2+}, respectively, as they are present as Fe^{2+} and Ni^{2+} in the respective electrolytes. Fig. 1b compares the formation potentials of various transition metal fluorides and $CF_{1.1}$ vs. Li^+/Li. Thermodynamically, it is feasible to synthesize all of the transition metal fluorides beneath the dotted line (Fig. 1b) by reacting CF_x with the respective transition metal. The feasibility of such a process depends mainly on two aspects: the reduction of CF_x with desired metal should be thermodynamically feasible and on the availability of suitable electrolyte that can transport and deliver the desired metal ions to the intercalation host. Fig. 1c represents the scheme adopted for the electrochemical synthesis of CMFNCs. Using this approach, we have synthesized C-FeF_2 and C-NiF_2 nanocomposites and tested them as cathode materials in rechargeable lithium batteries. In a typical CF_x/Fe cell, Fe metal will oxidize to Fe^{2+} at the anode and dissolves in the electrolyte. For charge balance, the Fe^{2+} from the electrolyte will be released to CF_x at the cathode. The electrons generated by the oxidation of Fe metal will travel through the external load, reach the cathode, and reduces the CF_x. First, Fe^{2+} will be desolvated at the surface of CF_x. The desolvated Fe^{2+} will then be intercalated into the CF_x layers. The intercalated Fe^{2+} will defluorinate the CF_x and nucleate the formation of FeF_2 particles and conductive carbon. The FeF_2 particles thus formed will be wrapped in the conductive carbon. Initially, the intercalation reaction is expected to occur at the surface, which then proceeds to bulk.

Electrochemical cells were constructed using CF_x as a cathode, iron-metal as the anode, and 1.0 M $Fe(ClO_4)_2{\cdot}xH_2O$ dissolved in acetonitrile as an electrolyte (dried under 3 Å molecular sieves before use to remove the water, which might originate from the dissolved $Fe(ClO_4)_2{\cdot}xH_2O$). Acetonitrile was chosen as a solvent due to its relatively low solvent donor number (DN) of 14.1 kcal mol^{-1}, aprotic nature, and large electrochemical stability window. The low solvent DN means reduced binding energy between the solvent and the cation, which is a prerequisite for the initiation of a desolvation process of metal ions at the surface of the electrode material.

The formation potential of CF_x and FeF_2 is 4.21 and 2.66 V vs. Li^+/Li. The formation potential of CF_x against Fe^{2+}/Fe is 1.55 V vs. Li^+/Li (Fig. 1b); hence the formation of FeF_2 from CF_x and iron metal is thermodynamically feasible. Fig. 2a shows the discharge profile of the CF_x/Fe cell. The results of four different CF_x/Fe cells are shown in Fig. S1 (see supporting information). The cells were discharged at a current density of 10 mA g^{-1} to −0.3 V. All four cells yield similar discharge profiles with minor differences in the discharge capacity. During the discharge process, the voltage dropped from the open-circuit voltage (OCV) of 0.4 V to −0.1 V. Then the voltage was raised to −0.05 V. This small drop and increase of voltage was also seen in CF_x/Li cells (Fig. 1a), and it could be due to the reduced resistance of the electrode due to the nucleation of conductive carbon formed by the reduction of CF_x. The average discharge potential of the cell was −0.1 V, which is much lower than the predicted equilibrium potential of 1.55 V. The large overpotential observed is consistent with CF_x/Li cells. The average discharge potential of CF_x/Li cell is 2.5 V, while the predicted voltage is 4.21 V. The large overpotential observed in discharge could be due to the sluggish diffusion of metal cations within the CF_x layers. The strong electrostatic force between negatively charged fluoride ions and positively charged cations might impede the diffusion of cations.

We have also tested the discharge behavior of CF_x/Fe cells in 1.0 M $Fe(ClO_4)_2{\cdot}xH_2O$ dissolved in tetrahydrofuran (THF) as an electrolyte (dried under 3 Å molecular sieves before use). The discharge profiles of two different CF_x/Fe cells tested in THF electrolyte are shown in Fig. S2 (see supporting information). Surprisingly, these cells did not show any significant capacity even when discharged down to −1.0 V. The solvent DN of THF is 20 kcal mol^{-1}. The higher solvent DN of THF (compared to ACN) might lead to the relatively strong binding between THF and Fe^{2+} and might not desolvated Fe^{2+} at the surface of CF_x. These studies might guide in choosing the right solvent for the electrochemical intercalation of transition metal ions.

Fig. 2b compares the XRD patterns of electrochemically synthesized C-FeF_2 with that of chemically synthesized C-FeF_2 nanocomposite (synthesized by reacting CF_x and $Fe(CO)_5$ at 250 °C [16]). The XRD patterns of electrochemically synthesized C-FeF_2 were directly collected on an electrode coated on stainless steel (SS) current collector. For comparison, the XRD pattern of the SS current collector was incorporated. The reflections marked with * are the main reflections of FeF_2 and matches well with the chemically synthesized FeF_2. The other strong reflections were due to the SS current collector. The XRD results provide direct evidence for the formation of FeF_2. Fig. 2c, d shows the SEM images of C-FeF_2 electrodes with different magnifications. Two different morphologies are evident from the SEM images. The bigger platelet-like particles are C-FeF_2, and the smaller spherical particles are conductive carbon used in the fabrication of the electrodes. No FeF_2 particles were seen on the surface of the platelets and confirm the confinement of FeF_2 within the carbon matrix. Fig. S3 shows the energy-dispersive X-ray (EDX) images of C-FeF_2 nanocomposites. From the elemental mapping, it is evident that Fe, F, and C were distributed uniformly. Fig. S4 shows the transmission electron microscopy (TEM) image and selective area electron diffraction (SAED) pattern of C-FeF_2 nanocomposites. TEM reveals the presence of nanocrystalline FeF_2 (5 to 10 nm in size) particles embedded uniformly in the carbon matrix. The dotted ED patterns further indicate the crystallinity of FeF_2 nanoparticles. For comparison, SEM images of pure CF_x (Fig. S5b) and chemically synthesized C-FeF_2 nanocomposites (Fig. S6) are given in supporting information. The morphologies of electrochemically synthesized and chemically synthesized nanocomposites appear to be similar.

From the above results and discussion, it is apparent that the formation of FeF_2 nanoparticles is a result of the intercalation of Fe^{2+} into CF_x layers. However, it could be hypothesized that the formation of FeF_2 nanoparticles is due to the surface reaction between CF_x and Fe^{2+}. From the discharge capacity of the CF_x/Fe cell (more than 800 mAh g^{-1}), it is clear that the full amount of CF_x is reacted. The surface reaction between CF_x and Fe^{2+} cannot explain the high capacity observed in CF_x/Fe cell. Further, from the SEM and TEM images, it is clear that the FeF_2 nanoparticles were well embedded in the carbon matrix. This indicates the reaction between Fe^{2+} and F^- occurred in the bulk of the CF_x. If there is a significant reaction at the surface, a large amount of FeF_2 particles would have formed on the surface. Further, to assume a surface reaction between F^- and Fe^{2+}, F^- should move to the surface of the CF_x. The carbon-fluorine bond in CF_x is covalent. Therefore, it is unlikely that F^- would move to the CF_x surface at RT. It is more likely that Fe^{2+} intercalated into CF_x layers and resulted in the formation of FeF_2.

Fig. 3a and b show the discharge-charge profiles of the C-FeF_2 electrode and its cycling behavior. The cells were cycled at 20 mA g^{-1}. The capacities were calculated with respect to the active material weight (FeF_2). The first discharge and charge capacities of the cell were 418 mAh g^{-1}, and 363 mAh g^{-1} with an irreversible capacity loss (ICL) of 55 mAh g^{-1}. The cells show a stable reversible capacity up to 15 cycles (353 mAh g^{-1}) and faded rather quickly to 297 mAh g^{-1} after

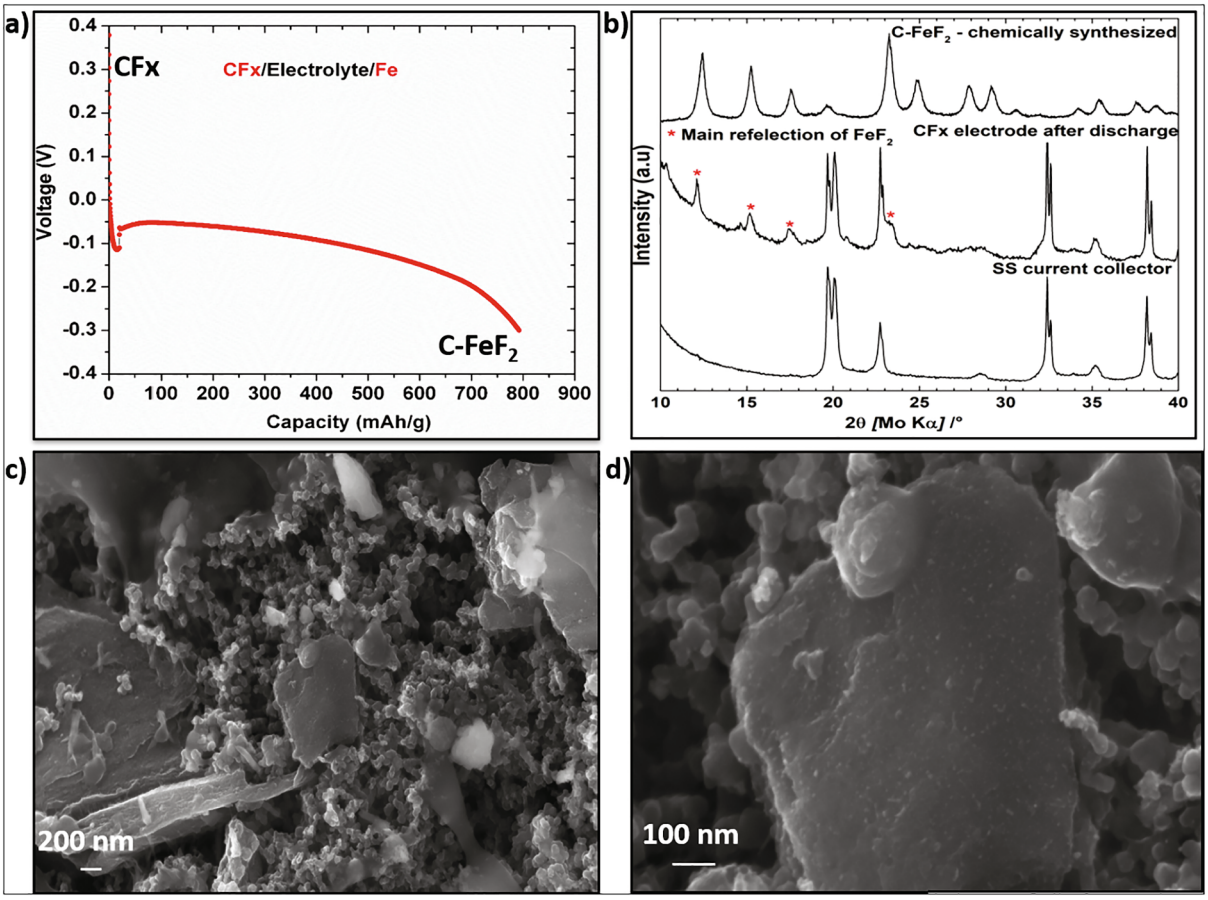

Fig. 2. a) discharge profile of CF_x/Fe cell; b) XRD patterns of stainless steel, electrode obtained after discharging the CF_x/Fe cell down to −0.3 V at 10 mA g^{-1}, chemically synthesized C-FeF_2; c) and d) SEM images of electrochemically synthesized C-FeF_2 nanocomposites at different magnifications.

40 cycles. Interestingly, the cycling performance of the electrochemically synthesized C-FeF_2 shows better stability than chemically synthesized C-FeF_2 (synthesized by reacting CF_x and $Fe(CO)_5$ at 250 °C [16]). The reversible capacity of chemically synthesized C-FeF_2 is 181 mAh g^{-1}, whereas electrochemically synthesized material is 349 mAh g^{-1} after 20 cycles. The theoretical specific capacity of FeF_2 is 571 mAh g^{-1}. However, we observed only 418 mAh g^{-1} in the first discharge. The low discharge capacity of electrochemically synthesized C-FeF_2 might be due to the leaching out of some FeF_2 particles from the electrode during the washing process of the electrode. Washing was performed with anhydrous acetonitrile to remove the electrolyte impurities from the CF_x/Fe cell.

The better cycling performance of electrochemically synthesized C-FeF_2 compared to chemically synthesized nanocomposites might be due to the homogeneous distribution of FeF_2 nanoparticles in the carbon matrix in the electrochemical method. In the chemical method, CF_x and $Fe(CO)_5$ were gradually heated in a closed Swagelok cell reactor at 250 °C for 24 h. In this reaction, initially, $Fe(CO)_5$ vaporizes at 105 °C

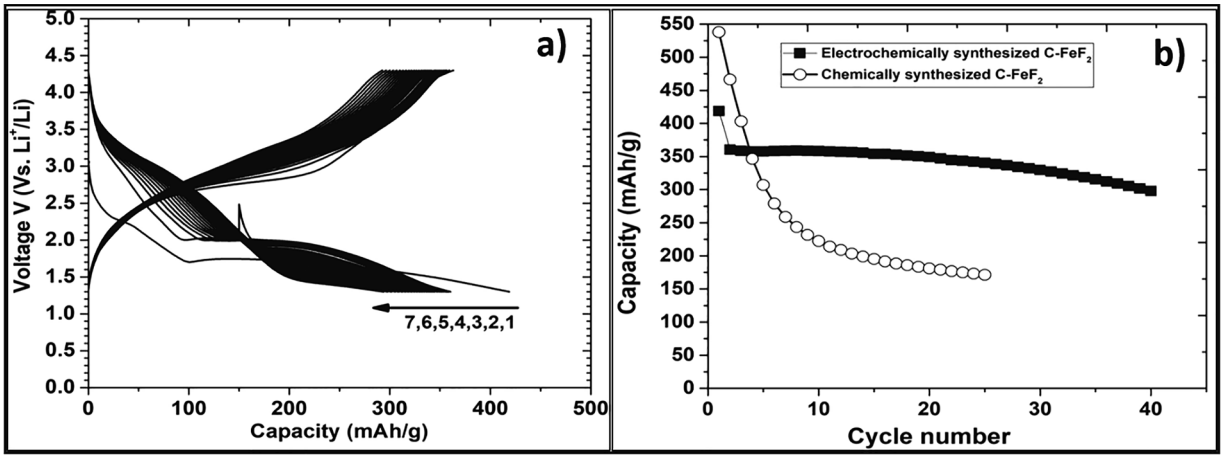

Fig. 3. a) shows the discharge-charge profiles of C-FeF_2 electrode obtained after discharging the CF_x/Fe cell, b) it's cycling behavior (the cycling behavior of chemically synthesized C-FeF_2 is included for comparison). The cells were cycled at 20 mA g^{-1}. Capacities are with respect to the active material FeF_2 weight in the composite.

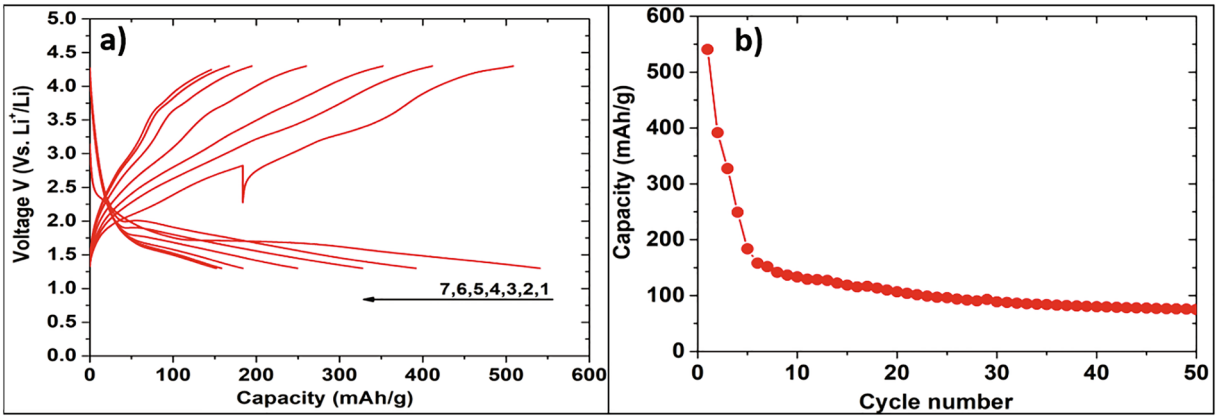

Fig. 4. a) shows the discharge-charge profiles of C-NiF_2 electrode obtained after discharging the CF_x/Ni cell, b) it's cycling behavior. The cells were cycled at 20 mA g^{-1}. Capacitates are with respect to the active material NiF_2 weight in the composite.

$(Fe(CO)_5$ gas will insert into CF_x layers under autogenous pressure), decomposes at 150 °C, and produces the iron nanoparticles. The iron nanoparticles will reduce the CF_x and from FeF_2 and conductive carbon at 250 °C [16,17]. These FeF_2 nanoparticles will be wrapped in carbon. As the final reaction occurs at 250 °C, there will be a certain amount of agglomeration of FeF_2 particles within the carbon matrix. In contrast to the chemical method, the electrochemical process occurs at RT and low current rates (10 mA g^{-1}). The kinetic energy available for the agglomeration of the FeF_2 particles is relatively low in this case and should allow better dispersion of FeF_2 crystallites within the carbon matrix. Therefore, the electrochemical method provided better control over the reaction and resulted in a suitable product for electrochemical applications. Homogeneous distribution of FeF_2 nanoparticles can better accommodate the volume changes that occur in the FeF_2 during discharge-charge reactions and reduces capacity fading.

To further validate this electrochemical method, we have synthesized C-NiF_2 nanocomposites similar to C-FeF_2 nanocomposites from CF_x. Fig. S7 shows the discharge profile of the CF_x/Ni cell obtained in 1.0 M $Ni(ClO_4)_2$ acetonitrile electrolyte. The average discharge potential of the CF_x/Ni cell is −0.3 V, 0.2 V less compared to that of CF_x/Fe cell. The low discharge potential of CF_x/Ni cell is due to the high reduction potential of NiF_2 compared to FeF_2 (Fig. 1b). The reduction potential of FeF_2 is 2.66, and NiF_2 is 2.94 V vs. Li^+/Li. This results in a low overall reduction potential of Ni/CF_x cells. Fig. 4a and b show the discharge-charge profiles of the C-NiF_2 electrode and its cycling behavior. In the case of C-NiF_2, the first discharge capacity was 540 mAh g^{-1}, close to the theoretical specific capacity of 554 mAh g^{-1} (Fig. 4a). However, in the case of C-NiF_2 capacity faded rapidly with cycling and reached a reversible capacity of 75 mAh g^{-1} after 50 cycles (Fig. 4b). We have not synthesized C-NiF_2 nanocomposite by the chemical method using nickel carbonyl and CF_x due to the high toxicity of nickel tetracarbonyl ($Ni(CO)_4$). Therefore, we could not directly compare the cycling performance of electrochemically synthesized C-NiF_2 and chemically synthesized sample. Nevertheless, the electrochemically synthesized C-NiF_2 nanocomposites showed better cycling stability compared to the chemically synthesized multiwalled carbon nanotube - NiF_2 nanocomposites reported by other authors [22].

4. Conclusions

We have demonstrated a new electrochemical method for the synthesis of carbon-metal fluoride nanocomposites. Electrochemical intercalation of Fe^{2+} and Ni^{2+} into CF_x led to the formation of C-FeF_2 and C-NiF_2 nanocomposites, which showed better electrochemical performance compared to the chemically synthesized C-MF_2 nanocomposites as cathode materials for lithium batteries. The electrochemical method described here is environmentally benign, cost-effective, occurs at RT, and extendable to synthesize several other CMFNCs and possibly to the electrochemical synthesis of carbon–metal oxides and carbon–metal sulphide nanocomposites. Such studies are under progress.

CRediT authorship contribution statement

M. Helen: Methodology, Investigation, Writing - review & editing. **Maximilian Fichtner:** Resources, Formal analysis, Writing - review & editing. **M. Anji Reddy:** Conceptualization, Writing - original draft, Formal analysis, Writing - review & editing.

Declaration of Competing Interest

The authors declare that they have no known competing financial interests or personal relationships that could have appeared to influence the work reported in this paper.

Acknowledgments

We thank and acknowledge Dr. V. S. K. Chakravadhanula for providing TEM images and Karlsruhe Nano Micro Facility (KNMF) for providing access to TEM facility. This work contributes to the research performed at CELEST (Center for Electrochemical Energy Storage Ulm-Karlsruhe). MF acknowledges partial funding by the German Research Foundation (DFG) under Project ID 390874152 (POLiS Cluster of Excellence).

Appendix A. Supplementary data

Supplementary data to this article can be found online at https://doi.org/10.1016/j.elecom.2020.106846.

References

[1] G.G. Amatucci, N. Pereira, J. Fluorine Chem. 128 (2007) 243–262.
[2] J. Cabana, L. Monconduit, D. Larcher, M.R. Palacin, Adv. Mater. 22 (2010) E170–E192.
[3] D. Andre, S.J. Kim, P. Lamp, S.F. Lux, F. Maglia, O. Paschosa, B. Stiaszny, J. Mater. Chem. A 3 (2015) 6709–6732.
[4] F. Badway, N. Pereira, F. Cosandey, G.G. Amatucci, J. Electrochem. Soc. 150 (2003) A1209–A1218.
[5] N. Pereira, F. Badway, M. Wartelsky, S. Gunn, G.G. Amatucci, J. Electrochem. Soc. 156 (2009) A407–A416.
[6] I. Plitz, F. Badway, J. Al-Sharab, A. Du Pasquier, F. Cosandey, G.G. Amatucci, J. Electrochem. Soc. 152 (2005) A307–A315.
[7] T. Li, L. Li, Y.L. Cao, X.P. Ai, H.X. Yang, J. Phys. Chem. C 114 (2010) 3190–3195.
[8] L. Li, F. Meng, S. Jin, Nano Lett. 12 (2012) 6030–6037.
[9] C. Li, L. Gu, S. Tsukimoto, P.A. van Aken, J. Maier, Adv. Mater. 22 (2010) 3650–3654.

[10] K. Rui, Z. Wen, Y. Lu, J. Jin, C. Shen, Adv. Energy Mater. 5 (2015) 1401716.
[11] Y. Lu, Z. Wen, J. Jin, X. Wu, K. Rui, Chem. Commun. 50 (2014) 6487–6490.
[12] Y. Lu, Z. Wen, J. Jin, K. Rui, X. Wu, Phys. Chem. Chem. Phys. 16 (2014) 8556–8562.
[13] R. Prakash, A.K. Mishra, A. Roth, C.h. Kübel, T. Scherer, M. Ghafari, H. Hahn, M. Fichtner, J. Mater. Chem. 20 (2010) 1871–1876.
[14] C. Wall, R. Prakash, C. Kübel, H. Hahn, M. Fichtner, J. Alloys Compd. 530 (2012) 121–126.
[15] F. Wu, V. Srot, S. Chen, S. Lorger, P.A. van Aken, J. Maier, Y. Yu, Adv. Mater. 31 (2019) 1905146.
[16] M. Anji Reddy, B. Breitung, V.S.K. Chakravadhanula, C. Wall, M. Engel, C. Kübel, A.K. Powell, H. Hahn, M. Fichtner, Adv. Energy Mater. 3 (2013) 308–313.
[17] B. Breitung, M. Anji Reddy, V.S.K. Chakravadhanula, M. Engel, C. Kübel, A.K. Powell, H. Hahn, M. Fichtner, Beilstein J. Nanotechnol. 4 (2013) 705–713.
[18] M. Anji Reddy, B. Breitung, C. Wall, S. Trivedi, V.S.K. Chakravadhanula, M. Helen, M. Fichtner, Energy Technol. 4 (2016) 201–211.
[19] M. Anji Reddy, B. Breitung, V.S.K. Chakravadhanula, M. Helen, R. Witte, C. Rongeat, C. Kübel, H. Hahn, M. Fichtner, RSC Adv. 8 (2018) 36802–36811.
[20] M. Anji Reddy, B. Breitung, M. Fichtner, ACS Appl. Mater. Interfaces 5 (2013) 11207–11211.
[21] J.L. Wood, R.B. Badachhape, R.J. Lagow, J.L. Margrave, J. Phys. Chem. 73 (1969) 3139–3142.
[22] Q. Huang, T.P. Pollard, X. Ren, D. Kim, A. Magasinski, O. Borodin, G. Yushin, Small 15 (2019) 1804670–1804681.